JOURNAL OF CATALYSIS 12, 45–60 (1968)

The Catalytic Oxidation of 1-Butene over Bismuth Molybdate Catalysts

IV. Dependence of Activity on the Structures of the Catalysts

PH. A. BATIST, A. H. W. M. DER KINDEREN, YVONNE LEEUWENBURGH, FRANCIEN A. M. G. METZ, AND G. C. A. SCHUIT

From the Department of Inorganic Chemistry, Technological University, Eindhoven, The Netherlands

Received March 6, 1968; revised April 25, 1968

A new method to prepare Bi_2O_3-MoO_3 catalysts consisting in boiling slurries of mixtures of freshly prepared and thoroughly washed bismuth hydroxide and molybdic acid has been developed. Catalysts prepared in this way are more active, more selective, and better reproducible than those obtained by other methods used earlier. These catalysts were investigated after various heat treatments by room-temperature X-ray analysis, infrared KBr wafer techniques, and reflection spectroscopy. Moreover their activities were determined for the 1-butene oxidative dehydrogenation. Superior catalytic activity appears confined to the compounds $Bi_2O_3 \cdot MoO_3$ (the low-temperature koechlinite modification) and $Bi_2O_3 \cdot 2MoO_3$. It is suggested that this activity is connected to the presence of corner sharing Mo–O octahedra in the bulk of the solid, that give rise to tetragonal pyramidal Mo–O sites at the surface also sharing only corners with neighbors. The promoting influence of Bi_2O_3 then might also arise because of forcing this structure on the MoO_3 component.

INTRODUCTION

Some time ago Bleyenberg, Lippens, and Schuit (*1*) published an investigation into the binary system Bi_2O_3-MoO_3, while Batist, Lippens, and Schuit (*2*) reported on the activities of Bi_2O_3-MoO_3 samples for the dehydrogenative oxidation of 1-butene to butadiene. The central point in these papers was an attempt to arrive at a description of the active site or sites at the surface of the bismuth molybdate catalyst. The answer to the problem remained somewhat obscure. There did not seem to be any connection between the presence of a particular compound and the catalyst activity: the only thing necessary seemed to be the simultaneous presence of both Bi^{3+} and Mo^{6+} in the catalyst. For several reasons it became advisable to reinvestigate the matter in more detail. Firstly, the work of Erman, Gal'perin, Kolchin, Dobrzhanskih, and Chernyshev (*3*) and of Blasse (*4*) has shown the phase diagram Bi_2O_3-MoO_3 to be more complex than assumed by us. Secondly, the method of catalyst preparation adopted by us following the literature appeared not particularly suitable for our object since it involved simultaneous changes in catalyst structure and of the surface area. It remained uncertain therefore whether changes in catalyst activity had to be ascribed to structural or to surface area changes. Finally, the kinetics of the reaction in so far as they were investigated by us proved more complex than expected from literature data and clearly needed a further investigation. We recently have discovered a new method of preparing bismuth molybdate catalyst that appeared to offer a number of advantages for our purpose.

Samples prepared in accordance with the new recipe showed better reproducibility, more activity, and even more selectivity. Since the catalyst formation occurred under well-defined conditions at a relatively low temperature, phase formation and sintering processes were better separated. The new catalyst type therefore seemed to offer a new possibility to reinvestigate the problem stated above. The present paper will report on surface area and structural transformation of some Bi_2O_3-MoO_3 catalysts as a function of temperature in relation to the catalytic activity. In a following paper we hope to report on the kinetics of the reaction.

EXPERIMENTAL PROCEDURE

Preparation of the Catalyst Used

Freshly precipitated, thoroughly washed $BiO(OH)\cdot H_2O$ and H_2MoO_4 were allowed to react in boiling water, while the total mass was stirred vigorously for 20 hr. Mixtures with Bi/Mo ratios of 2/3, 1/1, 2/1, 4/1, and 6/1 were subjected to this procedure.

The start of the reactions for mixtures with the ratios 2/3 and 1/1 was accompanied by a stiffening of the mass. Further boiling and stirring produced changes of color from white to yellow. The 2/3 sample remained almost white while the yellow color was strongest at the ratio 2/1 and moderate at the other ratios mentioned.

After reaction the solids were filtered and dried at 110°C for a night. Only traces of Bi and Mo ions were found to be left in the water filtrates.

Calcination of the Samples

Generally they were calcined in air at 500°C for 2 hr. Parts of the samples prepared in this way were further calcined at 600°C for 2 hr. In one case the time of calcination was 16 hr. In other cases higher calcination temperatures (680°, 750°C) were applied. The surface areas of the various samples, denoted further as E samples, were measured with an Areameter. They are given in Table 1.

Thermogravimetric Measurements

The calcination process was studied by use of a Stanton thermogravimetric balance. The results for some samples are represented in Fig. 1. It is shown that weight loss, i.e., dehydration, occurs in the temperature range below 500°C. This process is accompanied by a considerable decrease in the surface area (see Table 1). Increasing the calcination temperature to 600°C leads to a further decline in surface area, now, however, without loss in weight.

Differential Thermal Analysis Measurements

A few DTA measurements were made to ascertain whether phase changes could be detected during heating and cooling of some E samples. The apparatus used was the license CNRS model M-1 with platinum crucibles with α-Al_2O_3 heated to 1250°C as reference. The results are given in Fig. 2.

The situation for the $Bi_2O_3\cdot MoO_3$ sample appears relatively simple: there are two endothermic conversions, at 665° and 690°C. As shown later from X-ray data, it is here that the conversion of the low-temperature koechlinite form to the newly discovered high-temperature modification occurs. Why there are two transition points remains obscure. Cooling of the heated sample and subsequent reheating to higher temperatures does not show any heat effects: once the high-

TABLE 1
COLORS AND SURFACE AREA OF E SAMPLES[a]

Bi/Mo ratio	S (m^2g^{-1})						
	Dried at 110°C		Calcined at 500°C, 2 hr		Calcined at 600°C, 2 hr		600°C, 16 hr
2/3	wh	10.0	wh	2.0	wh	0.7	—
1/1	m.y	20.9	m.y	3.0	m.y	1.0	0.5
2/1(a)[b]	s.y	13.8	s.y	4.6	—	—	—
2/1(b)[b]	s.y	—	s.y	3.3	s.y	0.9	—
4/1	y	—	sl.o	8.7	—	—	—
6/1	sl.y	—	sl.o	5.7	—	—	—

[a] m, Moderate; s, strong; sl, slightly; wh, white; y, yellow; o, orange;
[b] a and b, preparation repeated.

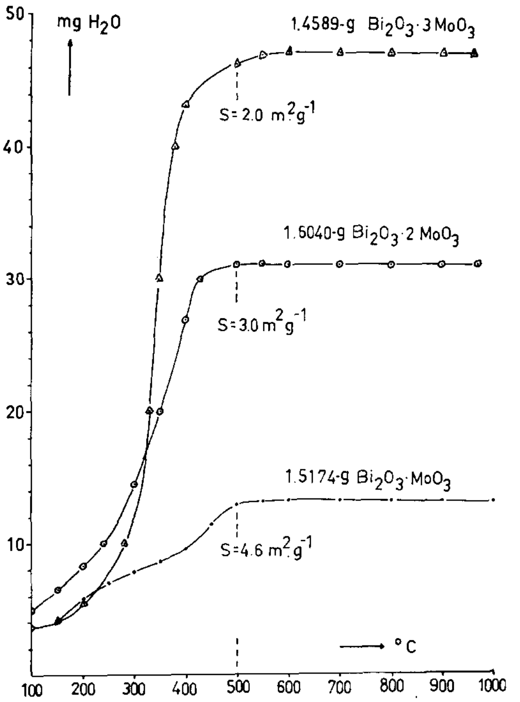

Fig. 1. The loss of water for some E samples measured with a thermogravimetric balance with a linear speed of 6°C min^{-1}.

temperature compound is formed it apparently remains stable.

Far more intricate is the situation for the $Bi_2O_3 \cdot 2MoO_3$ sample. If heated for the first time an endothermic transition is observed between 560° and 615°C; since from X-ray data it is found that at the latter temperature the sample consisted of the Erman $Bi_2Mo_2O_9$ phase this probably represents the conversion of $Bi_2O_3 \cdot 3MoO_3$ and $Bi_2O_3 \cdot MoO_3$ to $Bi_2O_3 \cdot 2MoO_3$. Around 665°C an exothermic process starts to develop that, however, is immediately followed by a sharp highly endothermic process at 690°C. At still higher temperatures there are signs for two exothermic conversions. Cooling the sample hereafter then showed two conversions as endothermic transitions but now more concentrated in their temperature range. At lower temperatures the situation is seen to be different from that encountered during heating: There are two pronounced exothermic conversions, at 659° and 632°C. The 659°C conversion may represent the solidification of the high-temperature 2/1 and the 2/3 modifications, the 632°C conversion the formation of the 1/1 compound. The phenomena observed during the first heating run could then perhaps be explained by first admitting an exothermic dissociation of the 1/1 compound to the high-temperature 2/1 and the 2/3 compounds, immediately followed by eutectic melting at 690°C. Although on the whole agreeing reasonably well with the X-ray data, the details of the conversion processes appear in need of further investigation.

Structure of Catalysts

Information concerning the presence of compounds and their possible structure be-

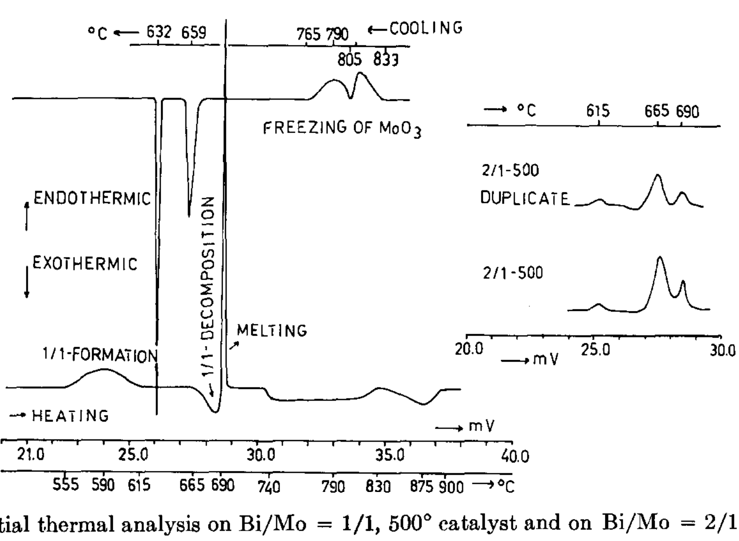

Fig. 2. Differential thermal analysis on Bi/Mo = 1/1, 500° catalyst and on Bi/Mo = 2/1, 500° catalyst.

fore or after heat treatment was derived from X-ray measurements, infrared measurements, and reflection spectroscopy.

1. *X-Ray Measurements*

X-Ray diagrams were obtained with a Philips X-ray diffractometer with Geiger-Müller counter and Ni-filtered Cu*K*α radiation.

a. $Bi_2O_3 \cdot 3MoO_3$. (See Table 2.) A sample dried at 120°C produced a diffraction pattern that was too vague to allow any identification. After preheating at 500° or 600°C the diagrams obtained closely resemble those given earlier by Bleyenberg *et al.* (*2*) and Erman, Gal'perin, Kolchin, Dobrzhanskih, and Chernyshev (*3*).

The diagram contains a multitude of lines pointing to a complicated structure. One strong line with $2\vartheta = 29.25°$ ($d = 3.05$) is characteristic and can be used for its identification. Our samples, like those produced by Bleyenberg (*2*) show a line at $2\vartheta = 16.8$ that is not given by Erman; it might belong to free MoO_3.

b. $Bi_2O_3 \cdot 3MoO_3$. (See Table 2.) Bleyen-

TABLE 2

X-RAY DIAGRAMS OF SOME CHARACTERISTIC E SAMPLES

$Bi_2O_3 \cdot 3MoO_3$ 600°C		$Bi_2O_3 \cdot 2MoO_3$ 600°C		$Bi_2O_3 \cdot MoO_3$ 600°C		$Bi_2O_3 \cdot MoO_3$ 750°C	
d	Int.	*d*	Int.	*d*	Int.	*d*	Int.
7.88	v.w	8.00	v.w	8.04	m		
6.90	m	6.62	w				
6.30	v.w						
5.94	v.w	5.95	m				
5.40	v.w	5.20	w			5.68	w
4.89	m.s	4.90	m				
4.54	w	4.74	m	4.44	v.w		
3.72	v.w	4.21	v.w	3.76	w		
3.57	m	3.99	v.w				
3.41	w	3.80	w				
3.315	w	3.55	v.w				
3.26	m	3.30	v.w			3.26	s
3.18	v.s	3.195	v.s	3.15	s	3.245	s
3.05	s	3.145	m				
2.87	s	2.975	v.w			2.87	m
2.79	m	2.80	s	2.74	s	2.79	m
2.50	w	2.70	m	2 69	m		
2.47	m			2.42	v.w		
2.27	v.w	2.195	v.w	2.27	v.w		
2.245	w	2.172	w				
2.005	m	2.043	v.w			2.005	m
1.96	w	1.990	m				
1.945	w	1.978	m	1.940	s	1.975	w
1.915	m	1.940	s	1.920	s		
1.850	v.w						
1.840	v.w						
1.830	v.w						
1.800	w						
1.765	w						
1.715	w					1.725	w
1.690	m	1.682	v.s			1.720	w
1.635	w	1.638	m	1.655	v.s	1.690	w
1.595	w	1.605	w	1.630	s	1.635	v.w
1.555	w	1.598	m	1.575	m.s	1.630	v.w
		1.593	w				

berg proved the existence of a compound that is identical in its diffraction pattern with the mineral koechlinite (K) as given by Zemann (*4*). Blasse (*5*) and also Erman showed that there exists a high-temperature modification of the same composition (K-II).

Samples with this composition were therefore preheated at various temperatures with the following results:

110°C. Diffuse diagram with a number of broad lines all identifiable as belonging to K.

500° and 600°C. Well-developed K diagram.

680° and 750°C. K-II diagram, in good agreement with the data of Blasse and Erman.

Our diffraction patterns of K-II are closely similar to those given by Blasse and Erman, with the exception that we find some of the lines, particularly the strong $2\vartheta = 27.3$ line, to be doublets with varying intensity.

c. $Bi_2O_3 \cdot 2MoO_3$. (See Table 2.) Previously we considered this composition to represent a mixture of K and the Bi/Mo = 2/3 compound with considerable formation of solid solution.

Erman demonstrated the presence of a phase with Bi/Mo = 1, stable at high temperatures. He found no evidence of mixed crystals. In view of the existence of this compound and moreover the possibility of a K $\rightarrow$ K-II conversion, the problem was reinvestigated. Firstly, mixtures of $Bi_2O_3 + MoO_3$ were melted at 1040°C and then suddenly cooled. The line diagram thus obtained proved to be similar to that of Erman. Apart from the lines they mention, we find a number of weaker lines at high *d* values. Subsequently, E samples of the composition Bi/Mo = 1 were preheated at various temperatures with the following results:

110°C. Diagram with broad lines, identifiable as belonging to K.

500°C, 2 hr and 4 hr. See Fig. 3. Mixture of Bi/Mo = 2/3 and K; no solid solutions. K-diagram considerably better developed than 2/3 pattern.

600°C, 16 hr. Table 2. See Fig. 3. Diagram similar to that of the 1/1 compound. No lines of 2/3 observable (absence of $d = 3.05$) and only traces of K lines.

750°C, 16 hr. See Fig. 3. Intricate pattern of lines that certainly reveal the presence of the 2/3 compound and the K-II compound ($d = 3.25$ Å) but also of the 1/1 compound.

1000°C, 16 hr, down to 750°C, 15 hr. Similar to above but 1/1 lines stronger and 2/3, but especially K-II lines, weaker.

Our suggestion of mixed crystal formation, previously made, now appears less probable

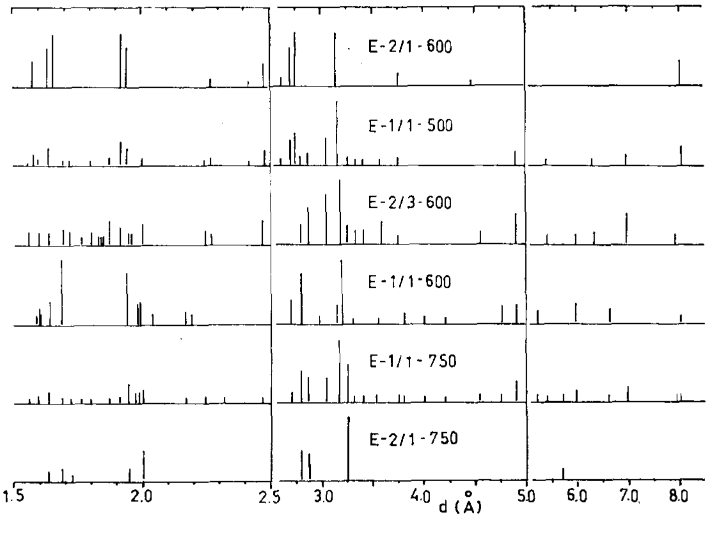

FIG. 3. Survey of X-ray diffraction patterns.

and possibly was caused by incipient formation of the 1/1 compound also in the old samples.

d. $2Bi_2O_3 \cdot MoO_3$ and $3Bi_2O_3 \cdot MoO_3$. Gattow (*6*) reported the formation of a compound at the composition Bi/Mo = 4/1 with CaF_2 structure, statistical distribution of the Bi and Mo ions over the cations sites, and vacancies at the anion sites. At 870°C this cubic structure is reported to transform into a tetragonal one.

Bleyenberg's DTA data gave no indication for the 4/1 compound but instead led to the proposal of the existence of the 6/1 compound ($3Bi_2O_3 \cdot MoO_3$). E Samples with compositions of $2Bi_2O_3 \cdot MoO_3$ and $3Bi_2O_3 \cdot MoO_3$ were prepared and studied. A low-temperature pretreatment (180°C) of $3Bi_2O_3 \cdot MoO_3$ (Fig. 4) produced a diagram of a hitherto unknown compound with broad lines. Pretreatment at 500°C produces a diagram that is different from but clearly closely connected to the K-II diagram with some splitting of its main reflections. Pretreatment at 750°C causes a further splitting of the K-II diffraction lines. Finally at 1000°C pretreatment the diagram becomes simpler again and now closely resembles that of K-II. From these data one might assume that in the high-temperature region there exist two modifications, that with a pattern as given by the 1000°C sample and another characterized by the 500°C sample; the 750°C sample apparently is a mixture of these two modifications.

The samples of $2Bi_2O_3 \cdot MoO_3$ (Figs. 4 and 5) pretreated at low temperatures (120° and 200°C) failed to produce the simple X-ray diagram as reported by Gattow. The diagram obtained showed the usual broad lines resembling the koechlinite pattern. Samples pretreated at 750°C were similar to the $3Bi_2O_3 \cdot MoO_3$, 750° pattern, however, even more intricate. The sample pretreated at 500°C (see Fig. 5), although mainly comparable to the general pattern of these samples with Bi_2O_3 in excess, showed some features that seemed more in accordance with the koechlinite diagram (see lines at d = 8.44, 2.72, and 2.49).

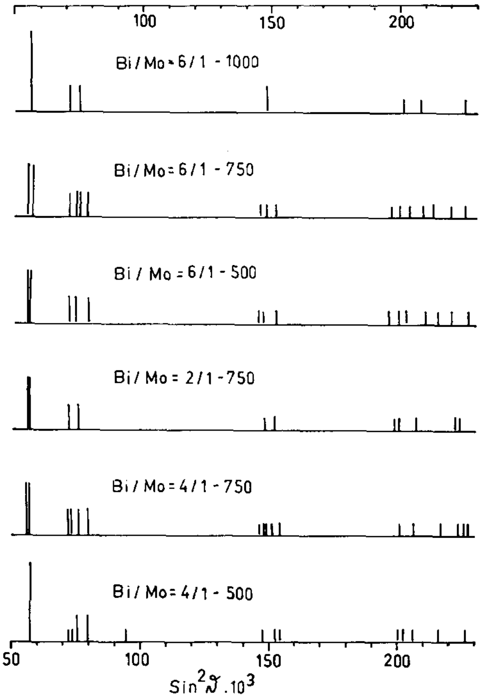

FIG. 4. Survey of X-ray diffraction patterns.

Generally speaking the diagrams obtained in the range Bi/Mo = 2–6 are derived from one type. The simplest form is given by the Bi/Mo = 6, 1000°C sample, that is almost

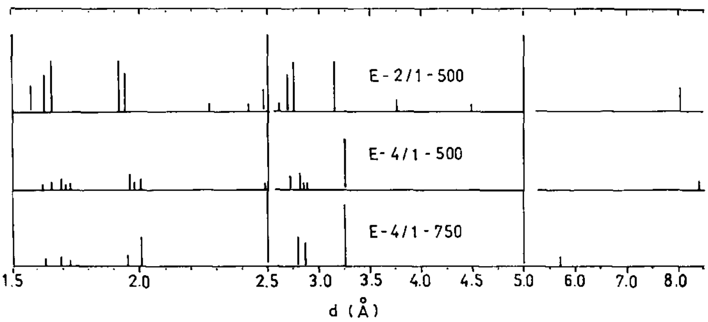

FIG. 5. Survey of X-ray diffraction patterns.

equal to the K-II diagram. A more intricate pattern still similar to the K-II is given by the Bi/Mo = 6–500°C sample.

All samples pretreated at 750°C appear to be mixtures, that of Bi/Mo = 6 obviously of the 1000°C and 500°C form. Finally the Bi/Mo = 4–500°C sample might be a mixture of a structure related to K-II with a small amount of a structure derived from K.

Rashkin and Pierron (*16*), who studied the structure of the $Bi_2O_3 \cdot 2MoO_3$ composition on Al_2O_3 by means of high-temperature diffraction, report that there occurs a formation of $2Bi_2O_3 \cdot MoO_3$ above 600°C and of exclusively $3Bi_2O_3 \cdot MoO_3$ at 750°C. This would infer either a loss of MoO_3 or its presence as an amorphous structure. They conclude from their measurements that X-ray data obtained at room temperature do not present an adequate picture of the situation at reaction temperatures. Although we have not performed high-temperature diffraction we feel not entirely convinced by their reports. Our main objection is that they do not state the nature of their X-ray diagrams after cooling since these should then be different from what they find at higher temperatures. It is, moreover, not clear to us how far they were aware of the existence of (1) the $Bi_2O_3 \cdot 2MoO_3$ structure and (2) of the high-temperature $Bi_2O_3 \cdot MoO_3$ modification. The latter point is particularly important in view of the similarity of the X-ray diagrams of the high-temperature $Bi_2O_3 \cdot MoO_3$ and the supposed compounds $2Bi_2O_3 \cdot MoO_3$ and $3Bi_2O_3 \cdot MoO_3$. Because of these objections we believe that the situation as concerns the significance of the room-temperature X-ray diagram is not so serious as they contend and we will proceed in considering them as relevant.*

2. Infrared Measurements

Infrared spectra of E samples, preheated at various temperatures, were obtained by the KBr disk techniques with the Perkin-Elmer Model 237 in the range 4000–625 cm^{-1} and Model 137 in the range 800–400 cm^{-1}. The results are given in Figs. 6, 7, and 8 and will now be discussed briefly.

Clark and Doyle (*7*) in a recent article on infrared spectra of molybdates and tungstates published the spectra of a number of these compounds, either having the metal ion in tetrahedral or in octahedral oxygen surroundings. The fundamental frequencies of tetrahedral anions in aqueous solution [see Busey and Keller (*8*)] are as follows:

MoO_4^{2-}:	894	407	833	318
Normal mode:	$\nu_1(A_1)$	$\nu_2(E)$	$\nu_3(F_2)$	$\nu_4(F_2)$

where the threefold degenerate ν_3 and ν_4 are infrared-active. In solids the position of the frequencies does not change considerably but lower site symmetries cause a splitting of the allowed infrared transitions and more-

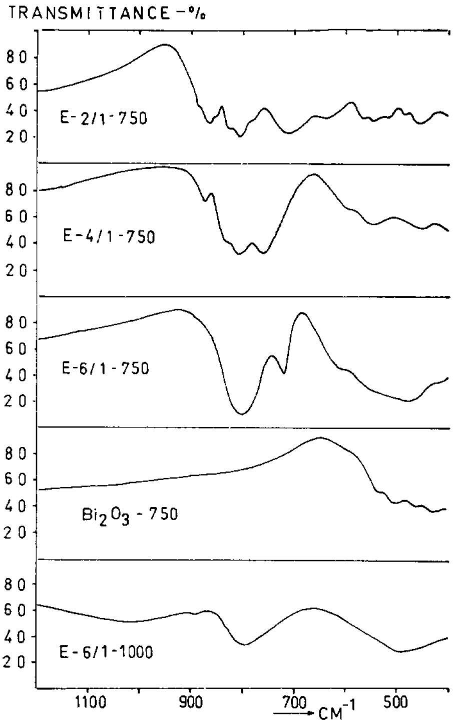

FIG. 6. Survey of infrared spectra.

---

* *Note added after completion of manuscript.* We are indebted to Prof. W. M. H. Sachtler for pointing out to us that X-ray measurements and DTA data were published by A. I. Gelbstein, S. S. Stroeva, N. V., Kul'kova Yu. M. Vashkin, V. L. Lapidus, and N. G. Sevast'yanov in a paper inaccessible to us [*Neftechimiya* **4**, 909 (1964)] but mentioned in L. Ya. Margolis, "Geterogennoe katalitischeskoe okislenie uglerodorodov" (Leningrad, 1967). From the data given in this book the B-phase $Bi_2O_3 \cdot 2MoO_3$ appears similar to that given by Erman *et al.* (13).

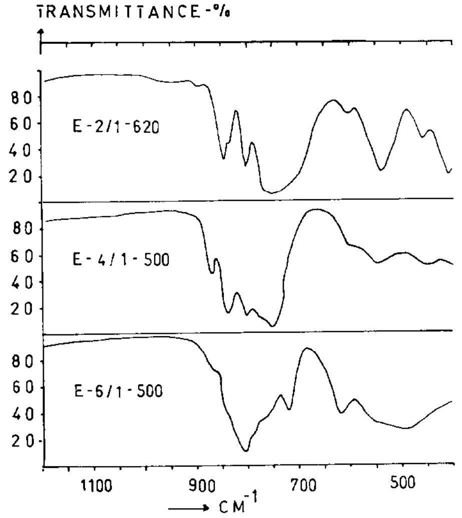

FIG. 7. Survey of infrared spectra.

over can cause the forbidden transitions to become weakly active. Nothing seems to be known about the fundamental frequencies of the octahedrally surrounded Mo ion in solution and since the low site symmetries in the solids cause extensive removal of degeneracy and the number of modes is larger the spectra are found to be more complicated than for the tetrahedral situation.

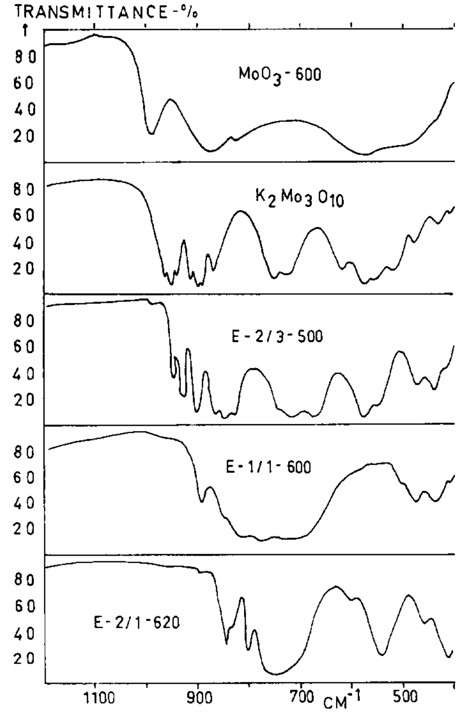

FIG. 8. Survey of infrared spectra.

The more simple spectra are found for samples with an excess of Bi_2O_3. Figure 6 for instance shows the spectra of $Bi_2O_3 \cdot MoO_3$, $2Bi_2O_3 \cdot MoO_3$, $3Bi_2O_3 \cdot MoO_3$, and Bi_2O_3 all preheated at 750°C and the spectrum of $3Bi_2O_3 \cdot MoO_3$ preheated at 1000°C. Bi_2O_3 produces a broad absorption band around 400 cm^{-1}. The $3Bi_2O_3 \cdot MoO_3$, 750°C sample also shows this absorption but on top of that a strong band at 805 cm^{-1}, a smaller band at 720 cm^{-1}, and what might be a band at 480 cm^{-1}. The 805-cm^{-1} band and the 500-cm^{-1} band can also be seen at the 1000°C sample but the 720-cm^{-1} band has now disappeared and a new shallow broad band at 1000 cm^{-1} has been formed. This band system develops into increasingly intricate patterns for $2Bi_2O_3 \cdot MoO_3$ and $Bi_2O_3 \cdot MoO_3$. Since the centra of the resonances seem to be present at the 800-cm^{-1} band that always dominates, it is proposed that the spectra represent the tetrahedral MoO_4^{2-} arrangement with $\nu_3(F_2)$ being the infrared-active mode that is split more or less because of lower site symmetries. The origin of the 480-cm^{-1} band is less clear; It might belong to the infrared forbidden $\nu_2(E)$ frequency and in fact seems to split into two bands at 550 and 450 cm^{-1}. If the 870-cm^{-1} band for the Bi/Mo = 2 and 4 ratios is ascribed to the forbidden $\nu_1(A)$ transition the band system could be understood completely as representing MoO_4^{2-} in tetrahedral configuration.

Figure 7 shows the spectra of Bi/Mo = 2, 4, and 6 for lower pretreatment temperatures. The koechlinite structure shows an entirely different spectrum than the K-II sample, there being bands at 850 (sharp), 800 (sharp), 760 (broad and intense), 600 (weak), 540 (intense), 460 (weak), and 410 (strong) cm^{-1}. The Bi/Mo = 6, 500°C sample however produces an almost identical spectrum as its 750°C pretreated counterpart.

The Bi/Mo = 4, 500°C sample is somewhat intermediate between the other two. One might therefore assume that the koechlinite spectrum represents the special octahedral surrounding accepted for this mineral, the Bi/Mo = 6 sample still indicates the tetrahedral situation, while the Bi/Mo = 4 sample is a mixture of the two.

Figure 8 shows the situation for Bi/Mo = 1 and 2/3 and for MoO_3. For reason of comparison the spectrum of $K_2Mo_3O_{10}$, known from X-ray measurements to possess chains of edge-sharing octahedra and tetragonal pyramids, is also given [see Gatehouse and Leverett (*10*)]. It is seen that the spectra become more and more complex the greater the excess of MoO_3. It is clearly impossible at this moment to ascribe the various transitions to the different octahedral modes. One might, however, account for the increasing complexity of the spectrum as a whole and in the range 900–1000 cm^{-1} in particular as originating from the combined influence of edge sharing of octahedra, double chains of corner-sharing tetrahedra and octahedra or tetragonal pyramids and octahedra. For instance, there is a close although not complete resemblance between $Bi_2O_3{\cdot}3MoO_3$ and $K_2Mo_3O_{10}$. Moreover, the spectrum of MoO_3 with a structure consisting of octahedra connected by edge sharing and corner sharing presents a strong band at 1000 cm^{-1}. $Bi_2O_3{\cdot}2MoO_3$ according to this assumption then should contain Mo–O octahedra without edge sharing and presumably only corner sharing. Its band structure is relatively simple, a weak sharp band at 895, a very broad and intense band between 830 and 700 cm^{-1}, and two weak bands around 450 cm^{-1}. Part of its Mo might be present as tetrahedra but a considerable fraction should be present as octahedra and then only in corner-sharing situations.

3. Diffuse Reflection

In view of the findings of Doyle and Forbes (*9*), who by the method of diffuse reflectance succeeded in demonstrating the presence of a number of compounds in the Bi_2O_3-MoO_3 system, some attention was given to the study of the diffuse reflectance of our samples mainly with the object of obtaining information on the surface layers. The measurements were made with the Zeiss Spectrophotometer P.M.Q.II with double monochromator MM 12 with quartz optics and photomultiplier 1 P 28. The angle of incidence of monochromatic light was 45°, intensity of radiation reflection measured perpendicular to the layer with MgO as the standard.

Diffuse reflectancies as obtained for some E samples as a function of the wavelength are given in Fig. 9. From curves of this type the "half wave number" $\sigma_{0.5}$ is calculated, being the wave number at which the light absorption was half that at the maximum. Two types of samples were investigated in this way, viz. D samples prepared by heating Bi_2O_3 and MoO_3 in various ratios for 48 hr at a certain temperature. Bi_2O_3 and MoO_3 were prepared by heating $Bi(NO_3)_3{\cdot}5H_2O$ p.a and $(NH_4)_6Mo_7O_{24}{\cdot}4H_2O$, respectively, for 48 hr at 500°C.

The E samples were prepared as described above.

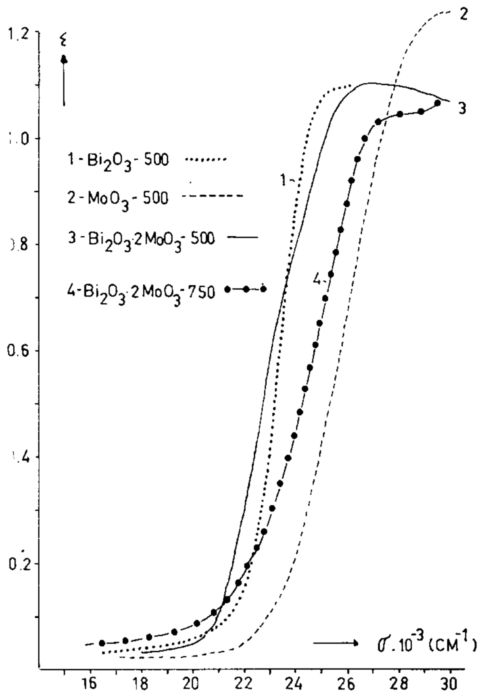

FIG. 9. Diffuse reflectancies for some oxides.

The dependency of $\sigma_{0.5}$ on composition for various temperatures of preheating has been given in Fig. 10. The conspicuous feature in this figure is the low $\sigma_{0.5}$ value for mixtures between Bi/Mo = 2/3 and 2/1 if preheated at 500°C. This is the reason for the yellow color of the samples in this range. Since the Bi/Mo = 2/3 compound is not yellow and in agreement herewith shows a

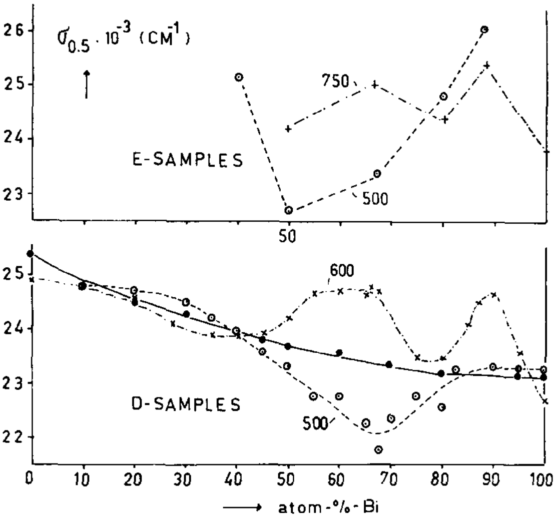

FIG. 10. Diffuse reflectance as function of composition.

relatively high $\sigma_{0.5}$ value and because it has been shown before that in this particular composition range the 500°C preheated samples are mixtures of 2/3 and K, the color apparently is caused by koechlinite. Preheating at 750°C destroys the color and also shifts $\sigma_{0.5}$ to higher values, in good agreement with the K → K-II phase change. One observation here however, appears, contrary to our former experiences: The 600°C preheated 2/1 sample shows the optical behavior of K-II while, as has been shown before and was also checked for this particular sample, the X-ray diagram was still that of K. Since diffuse reflection is especially connected with the surface layers of the crystal it therefore appears as if the K → K-II conversion occurs more readily at the surface than in the bulk of the crystal.

Rate Measurements

The apparatus for testing the activities of the catalysts was similar to that described in our former paper (*1*). The system of analysis of the gaseous products and the experimental conditions (e.g., the feed) were also the same, the only difference being the use of 2 g of catalyst instead of 2.5 g in a single run. In a special case with the same feed only 600 mg of catalyst was used. E Samples with different Bi/Mo ratios and preheated at various temperatures were investigated as to their activity and selectivity at constant GHSV and various temperatures. Conversions were expressed as reaction constants, assuming first order kinetics in the butene pressure and zero order dependency on oxygen and products pressure. The general impression obtained from experience with this catalyst type is one of considerably greater activity, equal or better selectivity, and better reproducibility.

As to their selectivity, the relative speed of conversion to CO_2 was similar to that with the older preparations but isomerization to 2-butenes was considerably slower. The *cis–trans* ratio of the 2-butenes was >1 at lower reaction temperatures, and became equal to 1 at higher temperatures. The improved reproducibility is reflected in the disappearance of the scatter in conversion for 1/1 samples as encountered earlier. The earlier reported concentration of oxidative dehydrogenation activity in the composition range Bi/Mo = 2/3–2/1 was also found for the E samples (see Fig. 11 for 500°C pretreated samples). The striking cessation of dehydrogenation activity at the ratio 4/1 is especially revealed in this figure. The influence of the temperatures on the rates will now be discussed.

Figure 12 shows the pseudo-first-order reaction constants for two samples of $Bi_2O_3 \cdot 3MoO_3$ preheated, respectively, at 500° and 600°C. A more or less "normal" behavior is observed, i.e., one could assume

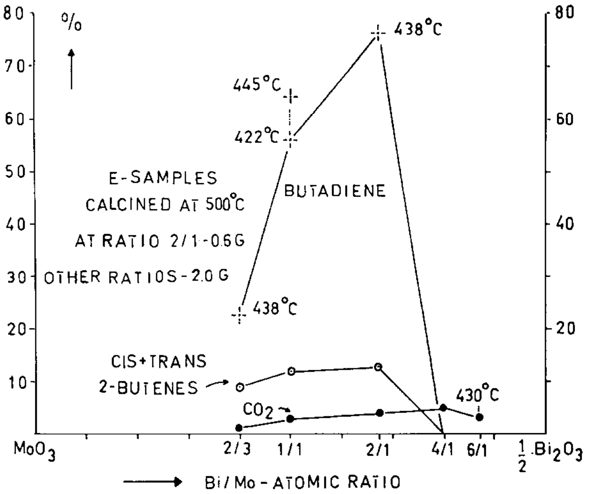

FIG. 11. Activity versus Bi/Mo composition for oxidation of 1-butene to butadiene (0.6 G, 2/1 phase; 2.0 G for the other phases).

that the data follow a simple Arrhenius law with an activation energy in the order of 16 kcal mole^{-1}. The decrease in activity with increasing pretreatment severity is approximately proportional to the decrease in surface area.

Figure 13 shows the rate constants as a function of the temperature for variously pretreated 2/1 samples. Two grams of the 500°C sample reacted so violently that it could only be measured without temperature peaks occurring in the reactor below 450°C. Above this temperature the catalyst became black during operation; it could be restored to its original yellow color and activity by a subsequent treatment with oxygen. It turned out that 600 mg of this catalyst was sufficient to reach the same conversions as obtained with portions of 2 g of other catalysts. In the region of low reaction temperatures a high activation energy in the order of 32–34 kcal mole^{-1} seems to appear. A preheating temperature of 600°C with 2 g of sample produced a catalyst somewhat less active than its 500°C preheated sample. The Arrhenius curves both show a definite break above 400°C.

The sample preheated at 680°C (conver-

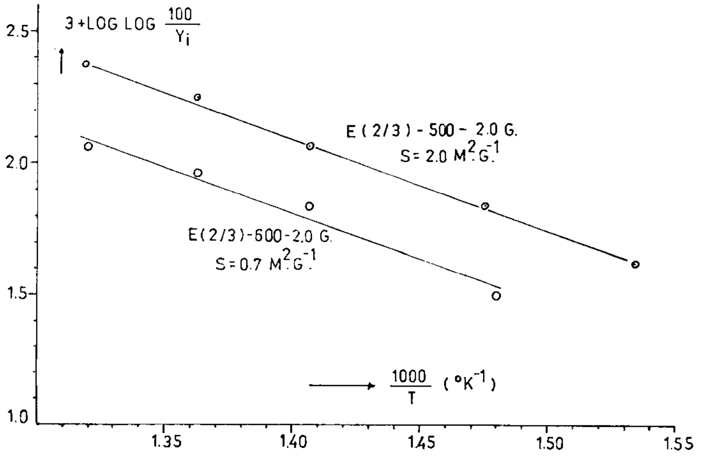

FIG. 12. Arrhenius plots of first order reaction constants vs. reciprocal temperature for reaction of 1-butene to give butadiene.

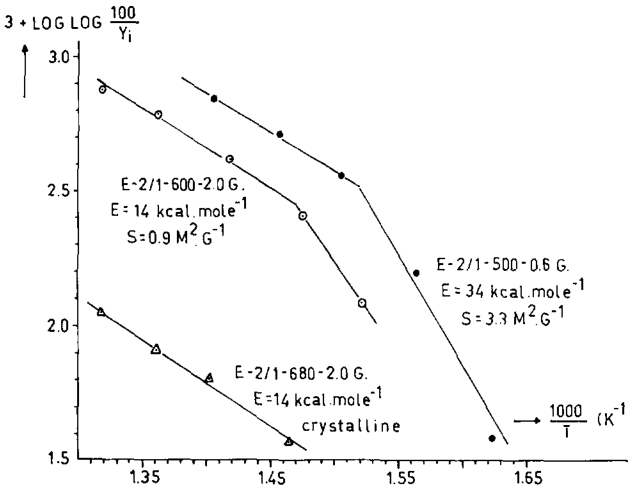

Fig. 13. Arrhenius plots of first order reaction constants vs. reciprocal temperature for reaction of 1-butene to give butadiene.

sion to K-II) is considerably less active but the activity per unit of surface area could not be less than that of the 600°C sample, its surface area being so low as to escape determination. From the straight line an activation energy around 14 kcal mole^{-1} is calculated.

Figure 14 finally illustrates the activities in their temperature dependency for Bi/Mo = 1 catalysts. The 500°C pretreated catalyst shows a curved Arrhenius line that could be reproduced by a mixture of the 2/1 and 2/3 samples in the correct ratio (Fig. 15). Interestingly enough the catalyst shows almost no change in color during operation. Pretreatment at 600°C for various times shows that the catalyst which is now in its $Bi_2O_3 \cdot 2MoO_3$ form is still highly active, an activity that is proportional to the surface area. In all cases the phenomenon of the curved lines remains present.

DISCUSSION

There seems to be little doubt that the exceptional catalytic activity of the Bi_2O_3-MoO_3 system is concentrated in the range 40–80 at. % Bi. The question that we shall now try to answer is whether this range

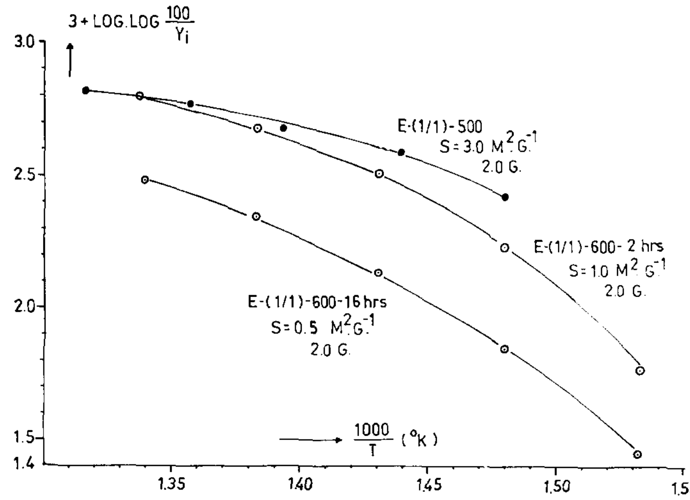

Fig. 14. Arrhenius plots of first order reaction constants vs. reciprocal temperature for reaction of 1-butene to give butadiene.

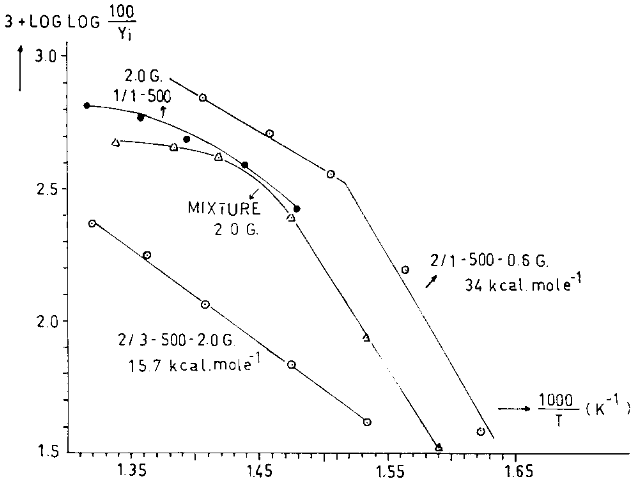

FIG. 15. Arrhenius plots of first order reaction constants vs. reciprocal temperature for reaction of 1-butene to give butadiene.

represents a special structural type or atomic configuration essential for the catalytic activity.

The X-ray evidence for the structure occurring in the Bi_2O_3-MoO_3 system is incomplete. It is known that the high-temperature Bi_2O_3 modification, stable above 720°C, is derived from a CaF_2 structure, the Bi^{3+} ions being surrounded by six oxygen ions in a situation derived from an eightfold cubic surrounding by removing two oxygen ions at positions diagonally opposite [Wells (*11*) p. 670]. It is believed that Mo^{6+} may replace the Bi^{3+} in this lattice with simultaneous occupation of the anion vacancies by O^{2-}. The limit of this replacement would be given by the composition $Bi^{3+}_{2/3}Mo^{6+}_{1/3}\cdot O^{2-}_{2}$, i.e., at Bi/Mo ratio = 2. However, Blasse has shown that the high-temperature modification of this composition possesses a La_2MoO_6 structure and hence consists of alternating $(Bi_2O_2)^{2+}$ layers similar to those encountered in BiOCl and layers of separate MoO_4 tetrahedra; a structure further denoted as $(Bi_2O_2)^{2+}(MoO_4)^{2-}_{t}$. The infrared and X-ray data obtained by us seem to indicate that in the range Bi = 80–85 at. % the structures occurring are related hereto and preserve in particular the MoO_4 tetrahedra. There is no actual evidence how the excess Bi_2O_3 becomes incorporated in the $(Bi_2O_2)^{2+}(MoO_4)^{2-}_{t}$ system. One possibility is that layers of $(Bi_2O_2)^{2+}O^{2-}$ comparable to $(Bi_2O_2)^{2+}Cl^{2-}$ with 2 Cl^- ions replaced by one O^{2-} ion are interspaced between the $(Bi_2O_2)^{2+}(MoO_4)^{2-}_{t}$ layers. Zemann's proposal for the structure of the low-temperature Bi/Mo = 2 modification presents an alternative structural solution. In principle the $(Bi_2O_2)^{2+}$ layers are still preserved but Mo now occurs in an octahedral environment with corner sharing in the basal plane, the remaining O^{2-} ions being placed in the direction of Bi^{3+} ions. We shall denote this as $(Bi_2O_2)^{2+}(MoO_4)^{2-}_{oct}$. Evidence has shown that elements of this structural type may occur in the composition range up to 80 at. % Bi but their stability is certainly less than at 67%, i.e., the koechlinite composition.

Turning to the discussion of the compounds relatively rich in MoO_3 we have to deal with $Bi_2O_3\cdot 2MoO_3$ and $Bi_2O_3\cdot 3MoO_3$, the former being an excellent and selective oxidation catalyst while the latter is only weakly active although remaining selective in its actions.

Erman *et al.* (*3*) proposed a unit cell for $Bi_2O_3\cdot 2MoO_3$ with $a = b = 11.8$ and $c = 5.4$ Å. In a subsequent note Erman and Galpernic (*13*) modified their unit cell dimensions to $a = 10.79$, $b = 11.89$, and $c = 11.86$ Å, hence apart from a slightly orthorombic distortion a cell with one of its dimensions multiplied by 2. The X-ray diagrams obtained by us for the $Bi_2O_3\cdot 2MoO_3$ compound are related to but not identical to those given by Erman *et al.* They might perhaps be indexed assuming an extremely long *c* axis of 54 Å, i.e., 5 times the value given by Erman. As a consequence of this long *c* axis the diagrams are richer in lines at low ϑ values (see Table 2). However, we believe that this particular feature does not introduce a fundamentally different point group since the stronger reflections are identical to those given by the Russian authors. The question then becomes whether the local configuration can be deduced from the available data.

The infrared evidence appears to point to a highly symmetrical situation that is similar to that given by the koechlinite modification, hence Mo in octahedral configuration with corner sharing of the octahedra. This seems to be provisionally acceptable judging from the X-ray data. If accepted as a working model the $Bi_2O_3 \cdot 2MoO_3$ structures than should consist of $(Bi_2O_2)^{2+}$ layers connected to a double layer of Mo–O octahedra, sharing corners in the *bc* plane and also between the two layers, i.e., a ReO_3 structure in the layers. Similar structures have been proposed by Aurivillius (*12*) for Bi_3NbTiO_9 and related compounds. The double layers are here constructed from Nb–O and Ti–O octahedra connected to a Bi_2O_2 layer. The remaining Bi^{3+} occupies a twelve-coordinated site and the ReO_3 assembly then becomes a perovskite structure. It is interesting to note that Aurivillius also introduces a long *c* axis of the order of 25 Å. Although therefore the evidence is mainly circumstantial we nevertheless suggest that the constructional principle in the $Bi_2O_3 \cdot 2MoO_3$ catalyst is again the Bi_2O_2 layer now connected to two corner-sharing Mo–O octahedra possibly forming double layers.

No attempt has been made so far at defining a structure for $Bi_2O_3 \cdot 3MoO_3$. However, the infrared evidence suggests that in this compound the usual situation prevalent in MoO_3-rich compounds, viz., an interlinking by edge sharing of Mo–O octahedra, is present. We know that this building principle also occurs in MoO_3 that possesses only weak oxidation activities.

We arrive therefore at the following hypothesis:

The presence of catalytic activity for the selective oxidation of olefins is connected with the presence of corner-sharing Mo–O octahedra while it is largely absent in compounds containing edge-shared octahedra.

In other words the limit of catalytic activity at the Mo-rich side of the Bi_2O_3-MoO_3 binary system is given by the changeover from corner-shared to edge-shared Mo–O octahedra.

Additional support for this hypothesis is given by results reported earlier [Batist, Kapteyns, Lippens, and Schuit (*14*)] regarding the rate of reduction of nonstoichiometric Mo oxides by 1-butene. Of the compounds investigated, one—$Mo_{17}O_{47}$—proved outstanding in its reactivity to 1-butene, while the others—Mo_8O_{23}, $Mo_{18}O_{52}$, and Mo_4O_{11}—were far less reactive and comparable to MoO_3. Actually $Mo_{17}O_{47}$ according to Kihlborg (*15*) shows corner-shared polyhedra among which also occur octahedra.

We shall now have to discuss, assuming the presence of corner-shared Mo–O octahedra in the bulk crystal, which configurations can be expected to occur at the surface. Figure 16 gives a schematic picture of a $Bi_2O_2^{2+}$ = B layer and of a MoO_2^{2+} = A layer. In crystals they will be connected via layers of oxygen anions denoted by O. Schematically therefore

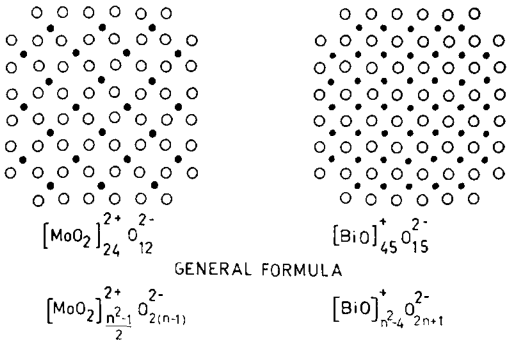

FIG. 16. Layer structure of bismuth molybdate.

(1) $Bi_2O_3 \cdot 2MoO_3 = (B\ O\ A\ O\ A\ O)_m$

(2) $Bi_2O_3 \cdot MoO_3 = (B\ O\ A\ O)_m$

(3) $2Bi_2O_3 \cdot MoO_3 = (B\ O\ A\ O\ B\ O)_m$ if octahedral.

Now, if we consider the A and B layers we shall have to decide about the situation at the edges. If these contain only O^{2-} ions the composition of a B layer will be $(Bi_2O_2)^{2+}_{\frac{1}{2}n}2\ O^{2-}_{2n}$ (n = number of O on edge) and of the A layer $(MoO_2)^{2+}_{\frac{1}{2}n}2\ O^{2-}_{2n}$ for n = great. Therefore the crystal would possess an excess of negative charge that has to be removed by leaving out edge O^{2-} ions or O^{2-} ions at the terminal O layer. Let us first consider cases (1) and (2). The terminal O layer consists actually of an assembly of Mo octahedra and so the O^{2-} ions are at the edges of the A layers. We will consider them as similar in first approximation. Leaving some of them out, i.e., introducing anion vacancies near to Mo ions, would lead to some of the boundary Mo ions being present in a tetragonally pyramidal 5-configuration that is not uncommon for Mo. Introducing an anion vacancy at the edge of a B layer would, however, bring the Bi^{3+} ion into a somewhat peculiar situation with three oxygens in a plane and close to the central cation while the two others are at a greater distance.

We shall therefore assume that (a) the anion vacancies are restricted to Mo^{6+} ions; (b) in accordance with an earlier suggestion (*1*) that these are the catalytically active sites.

Case (3), the $2Bi_2O_3{\cdot}MoO_3$ configuration, presents an interesting feature. Here the terminal O layer is not attached to Mo but to Bi. Contrary to the edge oxygens attached to Bi these can be removed easily: The Bi_2O_2 layer has been accepted already as being able to function as a terminal layer. The possibility therefore arises that here the anion vacancies are restricted to the terminal layer, leaving the edge Mo ions in full possession of their oxygen environment. In other words, the number of active sites is greatly reduced and an explanation is given of the cessation of the selective catalytic oxidation at Bi/Mo ratios greater than 2. Evidently, stripping the terminal O layer from the B layer introduces an inhibition of crystal growth. This, however, is also observable: The surface areas of the Bi-rich mixtures are greater (see Table 1) than those of the Mo-rich mixtures and so far the model is consistent. In itself this absence of catalytic activity might thus be considered as an indication of the validity of the site model proposed.

The second hypothesis proposed therefore is that the limit of catalytic activity on the Bi-rich side is given by the absence of anion vacancies connected to Mo, hence of tetragonally pyramidal Mo–O polyhedra as derived from corner-shared Mo–O octahedra. There still should be anion vacancies but these are now connected to Bi^{3+} and the catalyst therefore shows a type of oxidation catalysis that is peculiar for Bi_2O_3, viz., a slow oxidation leading to complete combustion.

From these points of view, the function of Bi is twofold. Following earlier suggestions, it acts because it can be reduced. Secondly, its presence enforces a structural situation on Mo–O that is particularly favorable for an interaction at the Mo ion. The model thus given possesses an interesting feature. We have shown before (*14*) that Bi-Mo catalysts are reduced by 1-butene in the absence of O_2 with an initial rate that is similar to the rate of the catalytic oxidation in the presence of O_2. In a more advanced state of reduction the rate is determined by the diffusion of O^{2-} from the interior to the surface. The activation energy of this diffusion is of the order of 30 kcal $mole^{-1}$, hence about equal to that encountered for the catalytic oxidation at the lower temperatures.

The suggestion therefore occurs that the catalytic oxidation always occurs via interaction with the oxygen of the solid. At the lower temperatures diffusion is slow and rate-determining while at the higher temperatures it is fast—as we found to be the case. The activation energy then encountered is that originating from the surface reaction. However, the consequences of this explanation are that we have to assume the reoxidation of the catalyst to originate at a different site than where the reduction catalytic activity resides. For instance, one could assume that reduction catalytic action occurred at the Mo terminal layers and O_2 uptake, hence reoxidation, at the Bi_2O_2 layers. An alternative and perhaps even more attractive possibility is that the oxygen is introduced into the bulk via the edges of the Bi_2O_2 and MoO_2 plates. Both the alternatives are pictured in Fig. 17.

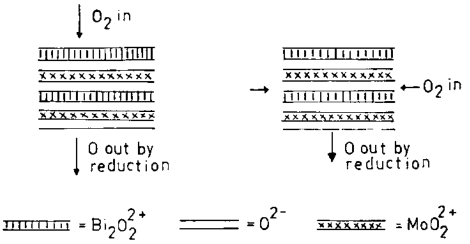

FIG. 17. Scheme for reduction and reoxidation of the catalyst.

One advantage of this model is that there is no competition any more between incoming hydrocarbon and O_2 for the occupation of the reactive site since the two processes occur on different sites. Consequent hereto we have no difficulty any more in explaining the generally observed zero order dependency on the oxygen pressure. Furthermore it is obvious that such a model would present a ready explanation for the excellent selectivity of the Bi molybdates. So far this model is nothing more than an *a priori* attractive but otherwise unproven possibility that is in need for further investigation. We hope to do this by a thorough inspection of the kinetics of the olefin oxidation.

ACKNOWLEDGMENTS

It is a pleasure to thank Miss J. L. M. Lebbink who performed the infrared measurements. We are grateful to Dr. J. L. Verbeek, Dr. B. C. Lippens, and Dr. A. H. W. M. der Kinderen for their suggestions concerning the diffuse reflectance measurements. We wish to express our gratitude to Prof. Dr. G. D. Rieck and Dr. K. Koopmans of the Physical Chemistry Department for their help given in the X-ray measurements and for the fruitful discussions with them concerning the structure analysis.

REFERENCES

1. BATIST, PH. A., LIPPENS, B. C., AND SCHUIT, G. C. A., *J. Catalysis* **5**, 55 (1966).
2. BLEYENBERG, A. C. A. M., LIPPENS, B. C., AND SCHUIT, G. C. A., *J. Catalysis* **4**, 581 (1965).
3. ERMAN, L. YA., GAL'PERIN, E. L., KOLCHIN, I. K., DOBRZHANSKII, G. F., AND CHERNYSHEV, K. S., *Z. Neorgan. Khim.* **9**, 2174 (1964).
4. ZEMANN, J., *Heidelberger Beitr. Miner. Petrogr.* **5**, 139 (1956).
5. BLASSE, G., *J. Inorg. Nucl. Chem.* **28**, 1124 (1966).
6. GATTOW, G., *Z. Anorg. Allgem. Chem.* **298**, 64 (1959).
7. CLARK, G. M., AND DOYLE, W. P., *Spectrochim. Acta* **22**, 1441 (1966).
8. BUSEY, R. H., AND KELLER, O. L., JR., *J. Chem. Phys.* **41**, 215 (1964).
9. DOYLE, W. P., AND FORBES, F., *J. Inorg. Nucl. Chem.* **27**, 1271 (1965).
10. GATEHOUSE, B. M., AND LEVERETT, P., *Chem. Commun.* **8**, 374 (1967).
11. WELLS, A. F., "Structural Inorganic Chemistry," 3rd ed. Oxford Univ. Press, London, 1962.
12. AURIVILLIUS, B., *Arkiv Kemi* **5**, 39 (1952); **1**, 463 (1949).
13. ERMAN, L. Y., AND GAL'PERIN, E. L., *Russ. J. Inorg. Chem.* **11**, 122, Jan. (1966).
14. BATIST, PH. A., KAPTEIJNS, C. J., LIPPENS, B. C., AND SCHUIT, G. C. A., *J. Catalysis* **7**, 33 (1967).
15. KIHLBORG, L., "The Crystal Chemistry of Mo Oxides," *Advan. Chem. Ser.* **39**.
16. RASHKIN, J. A., AND PIERRON, E. P., *J. Catalysis* **6**, 332 (1966).